

Visualization of Protein Interactions in Living Cells

Tomasz Zal

Department of Immunology, University of Texas, MD Anderson Cancer Center, Houston TX, USA

Ligand binding to cell membrane receptors sets off a series of protein interactions that convey the nuances of ligand identity to the cell interior. The information may be encoded in conformational changes, the interaction kinetics and, in the case of multichain immunoreceptors, by chain rearrangements. The signals may be modulated by dynamic compartmentalization of the cell membrane, cellular architecture, motility, and activation—all of which are difficult to reconstitute for studies of receptor signaling *in vitro*. In this paper, we will discuss how protein interactions in general and receptor signaling in particular can be studied in living cells by different fluorescence imaging techniques. Particularly versatile are methods that exploit Förster resonance energy transfer (FRET), which is exquisitely sensitive to the nanometer-range proximity and orientation between fluorophores. Fluorescence correlation microscopy (FCM) can provide complementary information about the stoichiometry and diffusion kinetics of large complexes, while bimolecular fluorescence complementation (BiFC) and other complementation techniques can capture transient interactions. A continuing challenge is extracting from the imaging data the quantitative information that is necessary to verify different models of signal transduction.

Introduction

Recognition of extracellular ligands by cell surface receptors depends on membrane compartmentalization, subcellular organization, and whole cell dynamics. Ligand-engaged or free receptors can interact with numerous proteins that co-inhabit the cell membrane, partition in different membrane domains, as well as being targets for intracellular adaptors, effector enzymes, cytoskeleton terminals, and the recycling machinery. Any of these interactions may modulate the activity of receptor components and all are themselves subject to continuous change according to subcellular localization, cell motility, polarity, state of activation, and the extracellular environment. Not surprisingly, the

mechanisms of ligand recognition by different receptors can be difficult to understand based on *in vitro* studies alone and have to be verified in the milieu of the living cell.

Particularly puzzling is the signal transduction by the multichain immunoreceptors that use dedicated chains for ligand binding and a number of noncovalently associated signaling chains to interface with the intracellular effector enzymes. How the information about the quality of binding between the ligand and the extracellular domain is projected by multichain receptors to the cell interior is of great general interest; especially for understanding antigen recognition, cytokine communication, and homeostasis in the immune system and beyond. According to the structural models, binding of a ligand to the extracellular domain induces a range of structural changes that propagate to the intracellular domains to expose sites for docking of various adaptors and signaling enzymes. The structural changes could be conformational, chain rearrangements, ligand-driven dimerization, or multimerization.¹ In contrast, the kinetic models favor the view that the information is conveyed by the net balance of otherwise unstructured interactions between the receptors and the membrane-resident kinases and phosphatases, which have opposing effects on signaling.² To distinguish between the alternative mechanisms requires quantitative characterization of various parameters of protein interactions in living cells. Verifying the structural mechanisms of ligand recognition requires determining distances and orientations between protein domains within and between receptors, while the kinetic models call for determination of affinities, lifetimes, diffusion coefficients, and frequencies of random collisions—all with subcellular resolution in living cells.

The last two decades witnessed significant refinement of fluorescence microscopy techniques that allowed looking non-invasively inside cells and visualizing receptor dynamics *in situ*. The most powerful approaches harness fluorescence to provide information about protein interactions (Fig. 1). The general strategy is to hyperlink the structural data on a pixel-by-pixel basis to additional parameters of fluorescence that are sensitive to the local environment. The most direct and versatile are imaging modalities based on Förster (fluorescence) resonance energy transfer (FRET), which is sensitive to the proximity and orientation between fluorophores and is amenable to the structural and the kinetic analysis. Complementary information about diffusion and stoichiometry of large protein complexes can be obtained by

*Correspondence to: Tomasz Zal; Email: tzal@mdanderson.org
Previously Published in: Multichain Immune Recognition Receptor Signaling: From Spatiotemporal Organization to Human Disease, edited by Alexander B. Sigalov. ©2008 Landes Bioscience and Springer Science+Business Media.
<http://dx.doi.org/10.4161/self.2.2.17932>

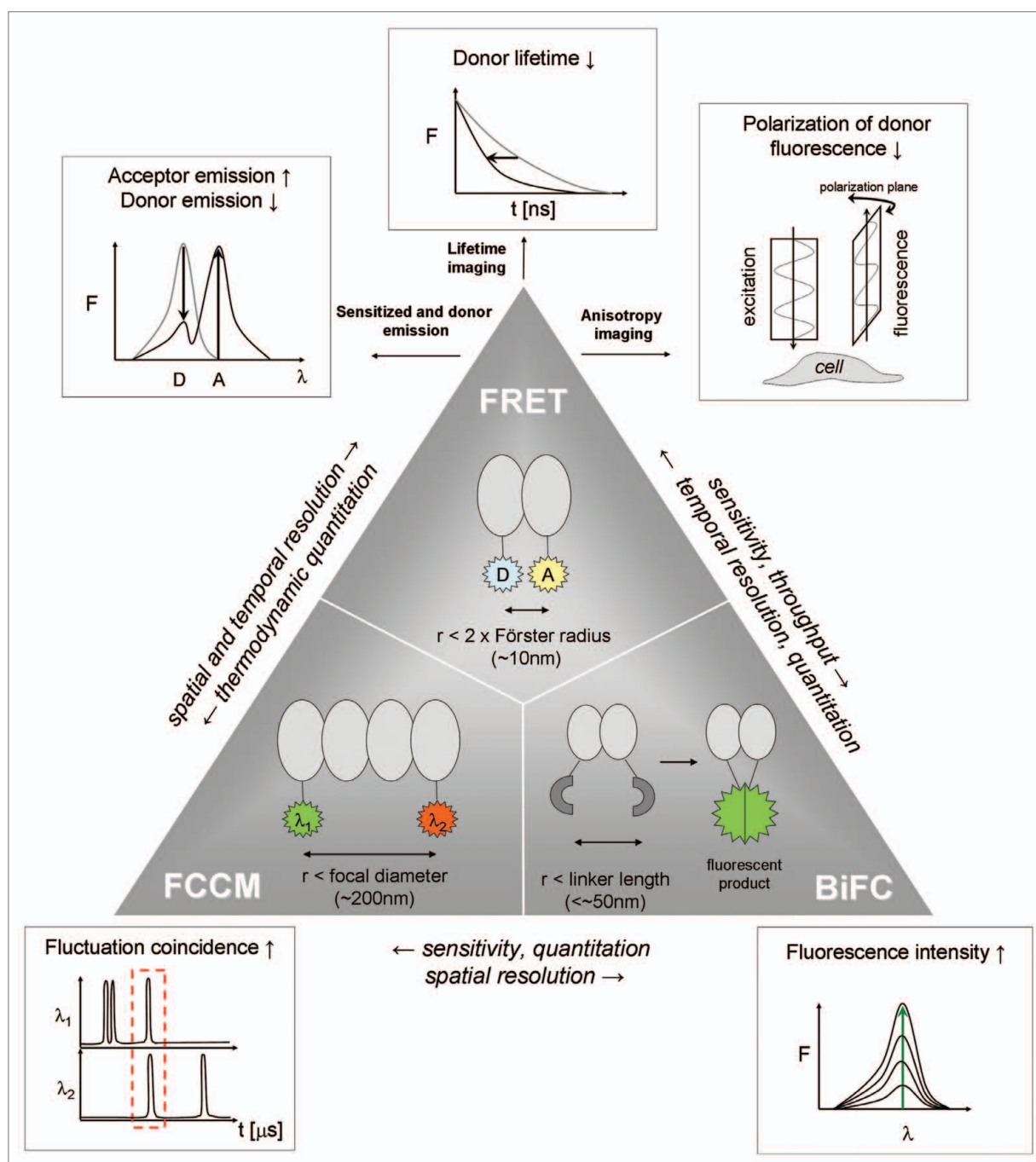


Figure 1. Major experimental approaches to quantitative imaging of protein interactions in living cells.

fluorescence correlation microscopy (FCM), while bimolecular fluorescence complementation (BiFC) and other complementation techniques can be used to determine protein interactions.

FRET

FRET microscopy is the most powerful and popular approach to study protein interactions in living cells. Occurring through dipole-dipole resonance between the excited donor fluorophore and a nearby acceptor, FRET allows direct detection of

nanometer-range proximity between appropriately labeled proteins as well as conformational changes. FRET can be imaged based on several parameters that are detectable by wide field, confocal, multiphoton, as well as total internal reflection fluorescence microscopy. Being a proximity effect, FRET can be used to detect both the specific complex formation as well as random collisions—both of which may be important for signaling by multichain immunoreceptors. We will focus later on how quantitative FRET imaging can be leveraged to study the underlying mechanisms of protein interactions.

Bimolecular Fluorescence Complementation

The BiFC technique is based on nonfluorescent, complementary fragments of fluorescent proteins (FPs) that can refold into a fluorescing product.³ By genetically attaching the fragments to different proteins, their interactions can be detected based on *de novo* fluorescence.⁴ Due to irreversible refolding, BiFC is not a general approach to monitor the dynamics of protein interactions but it excels as an end-point kinetic assay.⁵ Quantitative application of BiFC is possible by multiplexing fragments from different color FPs. That way, the relative efficiency of competing interactions can be evaluated ratiometrically.^{6,7} Recent improvements include new fragments of the Cerulean and Venus FPs that offer faster refolding kinetics and better sensitivity.⁸ The BiFC assay can complement FRET to determine and screen for protein interactions.⁹

Fluorescence Correlation Techniques

The formation of large protein complexes that exceed the nanometer range of FRET can be studied at the single-molecule level in living cells by FCM.¹⁰ This method uses highly sensitive detectors to detect bursts of fluorescence due to diffusion of single fluorophores through a small observation volume, which can come from a confocal or multiphoton excitation. The diffusion coefficient, which depends on the mass of freely diffusing complexes, can be discerned by applying the autocorrelation function to the fluctuations of fluorescence. Classic FCM is performed under free diffusion conditions to quantify the absolute molecular mass and the relative representation of the different weight species—in cells, it is best suited to follow interactions in the cytosol. Nevertheless, importantly to study membrane receptors, FCM is applicable to cell membranes as well.¹¹

FCM is robust only when detecting interactions of a small labeled ligand with a large partner. This limitation is avoided by labeling two proteins with different color fluorophores and enumerating the coincidence of diffusion, hence complex formation, by fluorescence cross-correlation microscopy (FCCM).^{12–16} FCCM is a powerful approach to directly measure the concentrations of the free and complexed species and from these, to calculate the affinity constant of complex formation in solution. Furthermore, the stoichiometry of the complex can be determined from the relative intensities during the coordinate bursts of fluorescence. By cross-correlating fluorescence in three or more colors, complex formation between more than two components can be studied.¹⁷ Recent advances in FCCM improved the sensitivity and cross-talk separation by using time- and space-correlated single photon counting as well as interleaved excitation.^{18,19} F(C)CM techniques are not suitable for full frame imaging, however, and are typically used for spot measurements in predetermined sites of the cell body. An imaging variant of FCM is achieved by cross-correlating fluorescence fluctuations across space instead of time; the technique is termed image cross-correlation microscopy (ICCM). ICCM allows imaging of the degree of aggregation and colocalization in living cells by confocal or multiphoton laser scanning.²⁰ As all fluorescence correlation techniques, ICCM performs well at low (physiological) concentrations of fluorophores but may require prolonged acquisition times.

Fluorescent Labeling of Proteins in Living Cells

Common to all techniques, the critical first step to visualizing protein interactions in living cells is fluorescent tagging of proteins with fluorophores that have suitable spectral properties and minimal impact on the biological functions. Foremost, proteins can be genetically fused with different color FPs that may be attached to the C or the N terminus or, if the structure of the carrier protein permits, spliced into the sequence of the protein.²¹ The growth of FRET imaging studies in living cells is particularly indebted to the development of FPs that are monomeric and have favorable spectral overlap, low cross-detection, high quantum yield, and low sensitivity of fluorescence to environmental changes.^{22–24} Currently, the recommended pairs of fluorescent proteins for FRET include mCerulean, CyPet, or SCFP3A as the donors and the yellow mVenus, mCitrine, or SYFP2 as the acceptors.^{23,25,26} Less often used but advantageous due to lesser photobleaching are the green-red pairs: EGFP as the donor and mRFP1, mKO, mOrange, or mCherry as acceptors.^{27,28} The nonfluorescent yellow chromoprotein REACh can be used as an acceptor-quencher with EGFP for lifetime and anisotropy-based FRET imaging.²⁹

The biggest drawback of FPs is their bulk, which may alter the cellular distribution or interfere with ligand binding. An alternative approach relies on small biarsenical fluorophores green FLAsH or red ReAsH that react specifically with short tetracysteine motifs, which can be incorporated at almost any place by genetic modification. A recent optimization of the tetracysteine motif improved the selectivity and lessened the conditions required for labeling in living cell.³⁰ For FRET, FLAsH and ReAsH can be acceptors for cyan FP and GFP, respectively.^{30–32} Additional possibilities for multiplexed labeling and pulse-chase studies are provided by attaching to the protein a binding domain that is specific for a small fluorophore. The O₆-alkylguanine-DNA alkyltransferase (AGT) domain can be labeled with fluorescent O₆-benzylguanine (O₆-BG) derivatives,^{33,34} oligohistidine sequences on cell surfaces can be labeled with nitroloacetate fluorophores,^{35,36} and acyl carrier protein (ACP) can be labeled with acyl-fluorophores.³⁷ Highly fluorescent nanocrystals (quantum dots) are advantageous for imaging of low abundance cell surface proteins and for FRET thanks to their brightness and good spectral separation of emission from excitation (Stokes shift).^{38,39} These and many other fluorophores can be attached to cell surface proteins in living cells using antibodies that do not interfere with biological functions. In permeabilized cells, imaging FRET between GFP-tagged receptors and fluorescent-labeled anti-phosphotyrosine antibodies allowed specific detection of receptor phosphorylation.^{40–42} A more extensive review of different classes of fluorophores and dyes suitable for FRET experiments is provided by Sapsford et al.⁴³

Quantitative FRET Imaging

Determining the efficiency of FRET is the key to analyze the structures and kinetics of protein interactions. FRET efficiency depends on the distance between donor and acceptor, as well as

the relative orientation of the electrical dipoles, the spectral overlap of donor emission with acceptor absorption, and the refractive index of the medium. In principle, one could triangulate the topology of multiprotein complexes by attaching donors and acceptors at various positions, measuring efficiencies of FRET, and calculating the distances according to the Förster equation. (The orientation factor (K^2) is equal to 2/3 if the donor or the acceptor has freedom of rotation.) However, when imaging FRET in a heterogeneous population of donors and acceptors, a typical situation in living cells, an important distinction has to be made between the intrinsic FRET efficiency, which characterizes individual donor-acceptor pairs, and the apparent efficiency (E_{app}), which is actually measured by most techniques. E_{app} is a weighted average of intrinsic efficiencies for all donors in the measurement volume; therefore, a particular E_{app} value can be due to a combination of distances, orientations, and degrees of donor occupancy by acceptor, as well as it could be due to random collisions. While E_{app} of a heterogeneous population cannot be used to calculate the donor-acceptor distance, a systematic analysis of the dependence of E_{app} on the local concentrations of donors and acceptors can shed light on the mechanism of protein interactions, which will be discussed later.

FRET efficiency can be quantified based on the donor fluorescence intensity, lifetime, and polarization, as well as from sensitized emission of acceptors (if these are fluorescent)—each modality offers a different balance of sensitivity, speed, and quantitation.

Donor dequenching. FRET quenches donor fluorescence; therefore, the rebound of donor fluorescence after photobleaching of acceptors provides a straightforward means to measure E_{app} . The raw data consist of two images: donor fluorescence taken before (D_{before}) and after (D_{after}) acceptor photobleaching:

$$E_{app} = 1 - D_{before} / D_{after}$$

An alternative approach is to monitor the rate of donor photobleaching, which is decreased in presence of FRET.^{44,45} Since the range of apparent FRET efficiencies may be in the order of only a few percent, low noise, precise detectors, and strong signals are essential to obtain reliable data—the accuracy can be improved by gradual acceptor photobleaching.⁴⁶ Due to a finite time required to substantially eliminate acceptors, photobleaching methods are limited by cell motility and instrument drift. Accordingly, donor dequenching tends to be used primarily for fixed or immobile specimens. Despite limitations, donor dequenching is a robust method to image E_{app} and is often used to corroborate FRET imaged by other methods. Imaging of FRET by photobleaching has been applied extensively to study the subcellular regulation of immunoreceptor interactions.⁴⁷⁻⁵²

An elegant extension of the donor quenching approach takes advantage of photoactivatable GFP (PA-GFP),⁵³ which can be instantaneously activated by illumination with a 405 nm laser and accept FRET from cyan FP donors.⁵⁴ When photo-activated locally in a subcellular compartment, the spreading of FRET (detected by the drop of donor fluorescence) provides invaluable information about diffusion, stability of protein complexes, and the rates of dissociation and association.⁵⁴

Sensitized fluorescence imaging. Unlike donor dequenching, sensitized emission-based FRET imaging does not require harsh irradiation and can be performed repeatedly on live cells with a high temporal and three-dimensional resolution.⁵⁵⁻⁵⁸ Numerous methods evolved over the years that take advantage of sensitized emission to detect FRET. In general, the sample is illuminated at the donor excitation wavelength and the measurement (imaging) is done at the donor as well as the acceptor emission wavelengths or, the full emission spectra are collected. The latter approach is often termed spectral FRET. For heterologous FRET experiments (as opposed to the internal FRET in covalently linked donor-acceptor sensors), the acceptor concentration has to be accounted for, hence an additional exposure is taken to acquire the acceptor-only fluorescence. E_{app} is calculated on a pixel-by-pixel basis based on the three intensities that are linearly unmixed from any spectral overlap:⁵⁷⁻⁵⁹

$$E_{app} = S / (S + D + G)$$

where S is sensitized fluorescence, D , donor fluorescence, and the G parameter⁶⁰ can be calibrated by acceptor photobleaching,^{57,59} lifetime measurements,⁵⁸ or by using pairs of donor-acceptor constructs having different FRET efficiencies.⁶¹ Additional calculations allow determination of local stoichiometry of donors, acceptors, and FRET complexes.⁵⁸

In the non-imaging mode, sensitized emission FRET was applied to study receptor aggregation in platelets,⁶² interactions between antibody-labeled IL-1 receptors,⁶³ ligand-dependent rearrangements of IL-2 receptor subunits,⁶⁴ the multivalent structure of T-cell receptor (TCR),⁶⁵ as well as MHC-I-dependent^{66,67} and -independent⁶⁸ interactions between TCR and CD8. Quantitative FRET imaging based on sensitized emission allowed time-lapse, three-dimensional visualization of interactions between the TCR ζ chain and CD4⁵⁷ or CD8⁶⁹ in immunological synapses. MHC-II interactions were tracked in subcellular compartments by confocal sensitized emission FRET.⁷⁰ In B-cells, quantitative sensitized emission allowed dissecting chain interactions and the lyn kinase recruitment during B-cell receptor (BCR) activation.^{71,72} Sensitized emission FRET is perhaps easiest to implement using wide field microscopy but it is applicable to confocal detection as well as two-photon, near-field scanning, or atomic force microscopy.^{70,73-75}

Fluorescence lifetime imaging. FRET shortens the time donors spend in the excited state, which can be imaged by fluorescence lifetime imaging microscopy (FLIM).⁷⁶ Two FLIM modalities are available, using pulsed excitation with time-gated detection (time-domain) or modulated excitation with phase-shifted detection (frequency-domain). Time-domain FLIM, especially when using time and space-correlated single photon counting mode (TSCSPC), allows recording entire fluorescence decay profiles for each voxel in three dimensions.⁷⁷⁻⁷⁹ This is a distinct advantage of time-domain FLIM over all other FRET modalities because the fluorescence decay curves can be deconvolved into individual lifetime exponents that are proportional to E_{int} , which is the basis for distance determinations. The average lifetime is proportional to E_{app} .^{80,81}

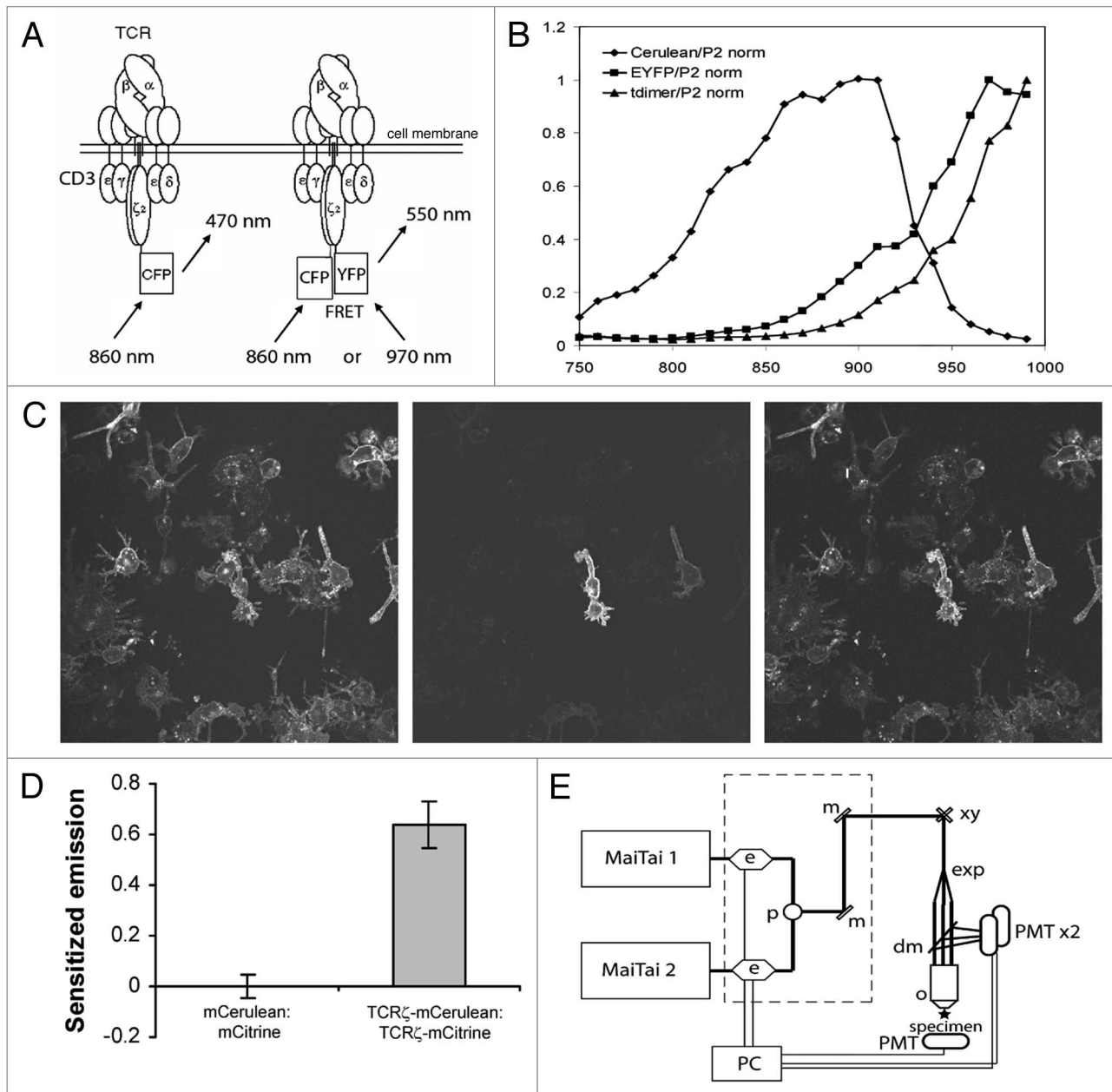


Figure 2. Imaging of heterogeneous FRET by dual laser, two-photon, interline excitation. (A) Experimental system to detect the proximity between the intracellular domains of T-cell Receptor (TCR) ζ chains. CFP denotes the mCerulean fluorescent protein. YFP denotes the enhanced yellow FP. (B) Normalized two-photon excitation spectra of CFP and YFP or CFP and the red fluorescent dimer(12) have poor overlap, which precludes efficient excitation at a single wavelength but allows selective excitation at 860 nm, 970 nm, and 990 nm, respectively. (C) Raw two-photon excited images of mCerulean, EYFP, and the raw FRET at the indicated excitation/emission wavelengths, respectively, in a mixture of T-cells expressing different ratios of TCR ζ -mCerulean and TCR ζ -EYFP. (D) Quantitation of donor-normalized sensitized emission in cells co-expressing donor and acceptor. Donor normalized sensitized emission (F_c/D) was calculated after subtracting the directly excited donor and acceptor signals from the raw FRET channel, as generally described for single photon FRET.⁵⁹ $F_c/D = (I_{860/550} - dI_{860/470} - aI_{970/550}) / I_{860/470}$. The cross-talk coefficients d and a were calibrated based on donor or acceptor only cells imaged under identical conditions. Non-interacting: co-expressed cytoplasmic (free) fluorescent proteins. (E) The optical path of the dual laser multiphoton microscope setup. MaiTai 1, 2: femtosecond lasers, e: electrooptical modulators, p: polarization merge optics, m: mirrors. xy: resonant scanner (Leica SP2 RS), exp: beam expander, dm: dichroic mirror, PMT: photomultiplier, o: water dipping objective (Olympus 20 \times NA = 0.95 or Leica 63 \times NA = 0.9). The figure is adapted from Zal et al, Proceedings of SPIE, with permission from the Society of Photo-Optical Instrumentation Engineers 2007.¹⁰³

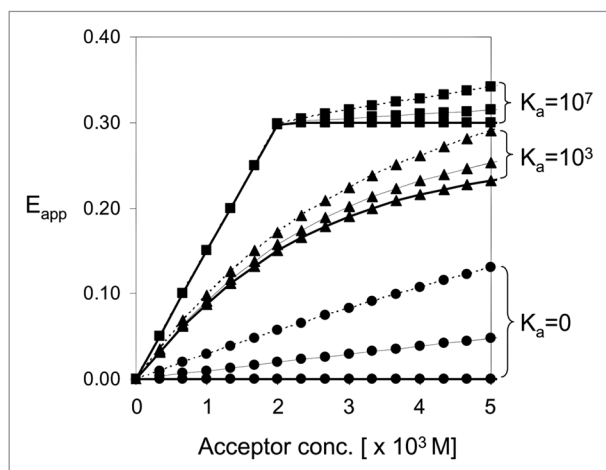


Figure 2. Modeling of the FRET dependence on the acceptor concentration for concurrent processes, formation of specific complexes and diffusion-driven random collisions. The model was derived by combining the Stern-Volmer equation for collision quenching with the affinity constant and the fluorescence lifetime—FRET efficiency relation. Assuming a 1:1 stoichiometry and donor concentration 2×10^{-3} M. Squares: a high affinity interaction, $K_a = 10^7$, triangles: a low affinity interaction $K_a = 10^3$, dots: no affinity, $K_a = 0$. Solid lines: no collisions, dashed lines: an intermediate rate of random collisions, dotted lines: a high rate of random collisions.

$$E_{\text{int}} = 1 - \tau_i / \tau_0 \quad E_{\text{app}} = 1 - \bar{\tau} / \tau_0$$

where τ_0 is the lifetime of free donors.

Important for the development of FRET imaging in vivo, time-domain lifetime imaging is an excellent match for multiphoton, femtosecond-pulsed excitation.^{82–85} Frequency-domain FLIM offers improved temporal resolution but is limited to average lifetimes,^{42,76,86} except when using more advanced, non-sinusoid modulation⁸⁷ or two-component analysis.⁸⁸ Acquisition times may be shortened by using a streak camera-based detection that can be combined with multiphoton excitation.^{83,89} In practice, however, a compromise is necessary between the temporal, spatial, and lifetime resolution. For this reason, application of FLIM to image fast interaction dynamics has been scarce. A general advantage of FLIM is the ability to detect FRET between spectrally similar donors and acceptors, in which case the combined donor and acceptor lifetime is increased.⁹⁰ Like all FRET imaging methods, FLIM has its caveats. One is the dependence of lifetimes on the refractive index around the fluorophore—the property that can be used to monitor the local environment in cells but can also interfere with the quantitation of FRET.^{91–93} Another difficulty is the sensitivity to photobleaching, which may be lessened by using GFP and mCherry instead of the more common CFP and YFP pair.²⁷

FRET imaging by polarization anisotropy. Yet another technique to image FRET is based on changes in fluorescence polarization anisotropy. The degree of fluorescence depolarization (in relation to the excitation light) depends on the rotational dynamics of the fluorophore and FRET.⁹⁴ Therefore, FPs are particularly suitable for polarization-based FRET imaging because, due to their large size, FPs are only minimally depolarized by the

rotational mechanism and all depolarization can be attributed to FRET. Fluorescence polarization anisotropy is calculated from the intensities of fluorescence that is detected through polarizing filters placed parallel (D_{\parallel}) and perpendicular (D_{\perp}) to excitation:

$$r = (D_{\parallel} - D_{\perp}) / (D_{\parallel} + 2D_{\perp})$$

Through additional calculations, polarization measurements can be converted to apparent FRET efficiencies.⁹⁵

Unlike other FRET imaging modalities, anisotropy imaging can detect FRET between fluorophores of the same type, obviating the need for double labeling with different donors and acceptors.^{96,97} This way, anisotropy imaging is particularly convenient to visualize homotypic aggregation and multimerization of FP-labeled proteins. Polarization FRET can be combined with lifetime microscopy for comprehensive characterization of rotational coefficients⁹⁸ or with sensitized emission to allow imaging of heterologous FRET in a single-exposure, which reduces motility errors.^{99,100} A minor drawback of polarization-based FRET imaging is somewhat lower spatial resolution and sensitivity due to using low numerical aperture objectives to maintain polarization.

Multiphoton imaging of heterologous FRET. Multiphoton microscopy has been used to image FRET based on donor lifetimes, polarization anisotropy¹⁰¹ and sensitized emission of acceptors.¹⁰² Nevertheless, due to single wavelength excitation, multiphoton-excited FRET could be imaged only when using internally linked biosensors but not in heterologous protein-protein interaction experiments, whereby donors and acceptors are attached to independently expressed proteins.

In heterologous experiments, FRET can result from molecular crowding and/or complex formation while no FRET can be due to a lack of interaction or insufficient acceptors. Therefore, regardless of the imaging modality employed to detect FRET, it is critical to account for the local acceptor concentrations that requires selective excitation at donor and acceptor specific wavelengths. By using dual, inter-line-switched femtosecond laser excitation and dual channel detection, we recently realized truly heterologous FRET imaging by multiphoton microscopy.¹⁰³ The system was tested using dimer-forming TCR ζ chains tagged with cyan and yellow FPs (Fig. 2).¹⁰³ Future application of sensitized emission multiphoton FRET imaging will be to study the motions of the intracellular signaling domains of TCR and other receptors at the sites of antigen exposure in vivo.

Using FRET to Analyze Receptor (Re)arrangements

Dimerization and multimerization of membrane receptors can be studied by co-expressing the receptors labeled with donor or acceptor and imaging FRET using any imaging modality.¹⁰⁴ For example, FRET images revealed differences in the oligomerization of B7-1 and B7-2 family members.¹⁰⁵ By fitting alternative mathematical models of molecule distribution to E_{app} , FRET can give insight into the spatial arrangement of clustered proteins.¹⁰⁶ Such analysis was applied to study IgA-ligand-receptor complexes

in the endocytic membranes in MDCK cells and indicated that single receptors in microclusters are surrounded by 2.5-3 neighbors. Similar quantitative FRET imaging confirmed multimerization of otherwise dimeric receptors of transferrin upon ligand binding,¹⁰⁷ dimerization of galanin-1 receptor,¹⁰⁸ and the dimer-tetramer transition of epidermal growth factor.¹⁰⁹

Internal rearrangements of multichain receptors were studied most extensively using cytokine receptors, whose signaling does not necessarily coincide with large scale clustering and is therefore more likely explained by conformational changes or chain rearrangements. Changes in the distance between the common signaling chain and ligand-specific chains were detected by FRET in IL-2 family receptors.⁶⁴ Likewise, in the case of the leukemia inhibitory factor receptor (LIFR), FRET between the LIF-specific chain and gp130 increased upon binding of LIF indicating ligand-induced heterodimerization or an intra-complex rearrangement.⁹ The latter possibility was supported by another study, which found that FRET between gp130 and LIFR was constitutive at the steady state and increased above the basal level upon LIF binding.¹¹⁰ An opposite effect was observed for the IL-17 receptor: FRET between intracellular domains of IL-17R (labeled with CFP and YFP) was constitutive at the steady state and decreased upon binding of IL-17.¹¹¹ The decrease indicated a scissor-like opening of the intracellular domains,¹¹¹ which was reminiscent of earlier observations in the interferon- γ receptor.¹¹² In the case of the IL-10 receptor, binding of IL-10 did not cause a change in FRET between the cytoplasmic domains.¹¹³ The homotypic lateral interaction between gp130 chains was studied in IL-6R using CFP and YFP fusions of gp130. FRET was constitutive and did not increase upon IL-6 ligation, which indicated that the gp130 chains in IL-6R are pre-associated and are not further cross-linked by IL-6.⁹ Ligand-induced internal rearrangements in BCR were also demonstrated by FRET.⁷¹ Largely undeveloped is the issue of the orientation of receptor domains with respect to the cell membrane, which may be tackled by introducing FRET donors or acceptors to the lipid environment.¹¹⁴

Imaging TCR-Coreceptor Interactions in the Immunological Synapse

According to the kinetic proofreading model of peptide-MHC recognition by TCR, generation of activation signals depends on a transient complex that needs to be stable enough to allow phosphorylation of CD3 chains by the Lck kinase. Lck is brought to the immunological synapse by CD8 or CD4 glycoproteins. Like TCR, these molecules can bind to MHC-I or MHC-II, respectively, and are brought in the vicinity of TCR coincident with TCR ligation.^{66,115} It was therefore possible that the dynamics of the interaction between TCR and coreceptors is regulated by the ligand quality. This hypothesis was tested by imaging FRET between the intracellular domains of TCR ζ -CFP (donor) and CD4-YFP (acceptor) using the sensitized emission method, which allowed three-dimensional time-lapse imaging of the immunological synapse and quantitation in terms of E_{app} . Indeed,

TCR ζ and CD4 are brought together as early as 30 s after T-cell encounter of agonist peptide-loaded antigen-presenting cells, i.e., before a cSMAC is formed, indicating that cSMAC formation is not prerequisite for the TCR-CD4 association.⁵⁷ Moreover, E_{app} was decreased in a dominant fashion by presentation of antagonist peptides that inhibit T-cell activation. A similar although not identical effect was observed between TCR ζ -CFP and CD8-YFP.¹¹⁶ The TCR ζ -CD8 associations were transient and had lower peak FRET efficiencies than the association of CD4 with TCR ζ , indicating a kinetic and/or structural difference between the ways CD8 and CD4 associate with TCR. Nevertheless, the kinetics of association between TCR ζ and CD8 in immune synapses correlated with the biological activities of presented peptides: agonists drove a fast raise of FRET and antagonists caused delayed FRET.¹¹⁶ Overall, FRET imaging supports the kinetic proofreading role of CD4 and CD8. However, it remains unclear to what extent exactly is FRET due to the formation of relatively stable complexes, i.e., affinity-driven interaction, or due to the regulation of diffusion-driven collisions in the immunological synapse.

Affinity versus Random Collisions: Acceptor Titration FRET

Irrespective which imaging modality is used to obtain quantitative FRET images, further analysis of the data, preferably in terms of FRET efficiency, is the key to study the mechanisms of protein interactions. Receptor signaling is often coincident with the clustering of receptors in a small area of the cell membrane; for example TCR in the immunological synapse, BCR cross-linking, or receptor clustering in lipid rafts. When using FRET to image receptor interactions, the question comes up on how to distinguish FRET due to the formation of specific complexes from FRET due to random collisions in the areas of receptor clustering.

In general, the strategy is to discriminate specific complexes from random collisions by titrating donors and acceptors and measuring local changes of FRET efficiency. For high affinity interactions, E_{app} is relatively independent of concentration (beyond stoichiometric acceptor concentration), while FRET due to random collisions will be evident only at a high local concentration of acceptor.^{117,118} The acceptor titration approach found extensive use to study how proteins are arranged in lipid rafts, which are submicrometer-sized assemblies of lipids and membrane proteins that are often involved in signaling. Titration analysis of FRET between raft-resident glycosyl-phosphatidylinositol (GPI)-linked fluorescent proteins showed that FRET depends on concentration, which is indicative of random interactions.¹¹⁹ More detailed analysis involved fitting alternative theoretical raft models to the observed relationship between apparent FRET efficiencies and concentrations of donors and acceptors.¹²⁰ The best fit was with the model where lipid rafts are small and harbor only several GPI-linked proteins in equilibrium with dispersed monomers. A poor fit was observed with models that assumed larger and more populous rafts. Concentration dependent FRET was also noted in other systems such as MHC-I, MHC-II, CD48, the

IL-2R/IL-15R subunits, or ErbB transmembrane receptor tyrosine kinases.¹²¹⁻¹²³ Some of these concentration effects could be attributed to partitioning in lipid rafts. Overall, these studies demonstrated that fitting the data to mathematical models is a powerful tool to distinguish complex formation from random interactions as well as to evaluate the distribution of receptors in membrane microdomains.^{124,125} Moreover, acceptor titration is also applicable to high throughput FRET screening to distinguish high affinity ligands in living (*E. coli*) cells.¹²⁶

Mathematical Model of FRET for Simultaneous Complex Formation and Random Collisions

It would be valuable to have a mathematical model to quantify FRET due to donors and acceptors forming specific complexes concurrent with interacting randomly due to diffusion-driven collisions. Both of these processes have been proposed to occur in immunological synapses. The frequency of random collisions can be characterized by the *bimolecular interaction constant* that is related to the diffusion coefficient in the Stern-Volmer equation of diffusion quenching of donor lifetimes.^{127,128} We modeled E in response to titration of donors by acceptors in solution by combining the Stern-Volmer equations with affinity and taking into account the relationship between donor lifetimes and FRET efficiency. **Figure 3** shows a family of analytical solutions for different affinities and diffusion kinetics. The model exhibits the

characteristic biphasic response of E_{app} . The initial raise in E_{app} is determined by the affinity constant, while the slope of E_{app} above the stoichiometric concentration reflects the bimolecular interaction constant. We envisage that by curve fitting the two-dimensional version of this model to the experimental data, it will be possible to evaluate the relative contribution of affinity and random collisions in membrane compartments as well. In general, continued development of acceptor (and donor) titration analysis will help in discriminating which mechanisms of protein interactions are modulated by ligand engagement.

Conclusion

Rapid development of quantitative imaging techniques allows non-invasive study of protein biochemistry in living cells. Arguably, a particularly promising approach is a combination of FRET imaging with computational modeling of FRET efficiency at different concentrations of donor and acceptor. Through such analysis, FRET imaging can be used to evaluate the affinity of complex formation and the frequency of diffusion-driven random collisions, both of which may contribute to signal transduction by multichain receptor complexes. Future developments will improve the quantitative analysis of FRET as well as applying other, complementary imaging approaches to uncover the structure and internal dynamics of cell surface receptors in living cells.

References

1. Sigalov A. Multi-chain immune recognition receptors: Spatial organization and signal transduction. *Semin Immunol* 2005; 17:51-64.
2. Davis SJ, Van der Merwe PA. The kinetic-segregation model: TCR triggering and beyond. *Nat Immunol* 2006; 7:803-9.
3. Ghosh I, Hamilton AD, Regan L. Antiparallel leucine zipper-directed protein reassembly: Application to the green fluorescent protein. *J Am Chem Soc* 2000; 122:5658-9.
4. Hu CD, Chinenov Y, Kerppola TK. Visualization of interactions among bZIP and Rel family proteins in living cells using bimolecular fluorescence complementation. *Mol Cell* 2002; 9:789-98.
5. Kerppola TK. Visualization of molecular interactions by fluorescence complementation. *Nat Rev Mol Cell Biol* 2006; 7:449-56.
6. Hu CD, Kerppola TK. Simultaneous visualization of multiple protein interactions in living cells using multicolor fluorescence complementation analysis. *Nat Biotechnol* 2003; 21:539-45.
7. Grinberg AV, Hu CD, Kerppola TK. Visualization of Myc/Max/Mad family dimers and the competition for dimerization in living cells. *Mol Cell Biol* 2004; 24:4294-308.
8. Shyu YJ, Liu H, Deng X, Hu CD. Identification of new fluorescent protein fragments for bimolecular fluorescence complementation analysis under physiological conditions. *Biotechniques* 2006; 40:61-6.
9. Giese B, Roderburg C, Sommerauer M, Wortmann SB, Metz S, Heinrich PC, et al. Dimerization of the cytokine receptors gp130 and LIFR analysed in single cells. *J Cell Sci* 2005; 118:5129-40.
10. Berland KM. Fluorescence correlation spectroscopy: A new tool for quantification of molecular interactions. *Methods Mol Biol* 2004; 261:383-98.
11. Schwille P, Korch J, Webb WW. Fluorescence correlation spectroscopy with single molecule sensitivity on cell and model membranes. *Cytometry* 1999; 36:176-82.
12. Bacia K, Majoul IV, Schwille P. Probing the endocytic pathway in live cells using dual-color fluorescence cross-correlation analysis. *Biophys J* 2002; 83:1184-93.
13. Kohl T, Heinze KG, Kuhlmann R, Koltermann A, Schwille P. A protease assay for two-photon cross-correlation and FRET analysis based solely on fluorescent proteins. *Proc Natl Acad Sci USA* 2002; 99:12161-6.
14. Kuroyama H, Ikeda T, Kasai M, Yamasaki S, Tatsumi M, Utsuyama M, et al. Identification of a novel isoform of ZAP-70, truncated ZAP kinase. *Biochem Biophys Res Commun* 2004; 315:935-41.
15. Hausteil E, Schwille P. Ultrasensitive investigations of biological systems by fluorescence correlation spectroscopy. *Methods* 2003; 29:153-66.
16. Bacia K, Kim SA, Schwille P. Fluorescence cross-correlation spectroscopy in living cells. *Nat Methods* 2006; 3:83-9.
17. Heinze KG, Jahnz M, Schwille P. Triple-color coincidence analysis: One step further in following higher order molecular complex formation. *Biophys J* 2004; 86:506-16.
18. Müller BK, Zaychikov E, Bräuchle C, Lamb DC. Pulsed interleaved excitation. *Biophys J* 2005; 89:3508-22.
19. Lamb DC, Müller BK, Bräuchle C. Enhancing the sensitivity of fluorescence correlation spectroscopy by using time-correlated single photon counting. *Curr Pharm Biotechnol* 2005; 6:405-14.
20. Wiseman PW, Squier JA, Ellisman MH, Wilson KR. Two-photon image correlation spectroscopy and image cross-correlation spectroscopy. *J Microsc* 2000; 200:14-25.
21. Rocheleau JV, Edidin M, Piston DW. Intrasequence GFP in class I MHC molecules, a rigid probe for fluorescence anisotropy measurements of the membrane environment. *Biophys J* 2003; 84:4078-86.
22. Shaner NC, Steinbach PA, Tsien RY. A guide to choosing fluorescent proteins. *Nat Methods* 2005; 2:905-9.
23. Giepmans BN, Adams SR, Ellisman MH, Tsien RY. The fluorescent toolbox for assessing protein location and function. *Science* 2006; 312:217-24.
24. Patterson GH, Piston DW, Barisas BG. Forster distances between green fluorescent protein pairs. *Anal Biochem* 2000; 284:438-40.
25. Rizzo MA, Springer GH, Granada B, Piston DW. An improved cyan fluorescent protein variant useful for FRET. *Nat Biotechnol* 2004; 22:445-9.
26. Kremers GJ, Goedhart J, van Munster EB, Gadella TW Jr. Cyan and yellow super fluorescent proteins with improved brightness, protein folding, and FRET Forster radius. *Biochemistry* 2006; 45:6570-80.
27. Tramier M, Zahid M, Mevel JC, Masse MJ, Coppey-Moisant M. Sensitivity of CFP/YFP and GFP/mCherry pairs to donor photobleaching on FRET determination by fluorescence lifetime imaging microscopy in living cells. *Microsc Res Tech* 2006; 69:933-9.
28. Peter M, Ameer-Beg SM, Hughes MK, Keppler MD, Prag S, Marsh M, et al. Multiphoton-FLIM quantification of the EGFP-mRFP1 FRET pair for localization of membrane receptor-kinase interactions. *Biophys J* 2005; 88:1224-37.
29. Ganesan S, Ameer-Beg SM, Ng TT, Vojnovic B, Wouters FS. A dark yellow fluorescent protein (YFP)-based Resonance Energy-Accepting Chromoprotein (REACH) for Förster resonance energy transfer with GFP. *Proc Natl Acad Sci USA* 2006; 103:4089-94.
30. Martin RM, Leonhardt H, Cardoso MC. DNA labeling in living cells. *Cytometry A* 2005; 67:45-52.
31. Hoffmann C, Galetta G, Bunemann M, Adams SR, Oberdorff-Maass S, Behr B, et al. A FIAsh-based FRET approach to determine G protein-coupled receptor activation in living cells. *Nat Methods* 2005; 2:171-6.

32. Nakanishi J, Takarada T, Yunoki S, Kikuchi Y, Maeda M. FRET-based monitoring of conformational change of the beta2 adrenergic receptor in living cells. *Biochem Biophys Res Commun* 2006; 343:1191-1196.
33. Keppler A, Gendreizig S, Gronemeyer T, Pick H, Vogel H, Johnsson K. A general method for the covalent labeling of fusion proteins with small molecules in vivo. *Nat Biotechnol* 2003; 21:86-9.
34. Keppler A, Arrivoli C, Sironi L, Ellenberg J. Fluorophores for live cell imaging of AGT fusion proteins across the visible spectrum. *BioTechniques*. 2006; 41:167-70,172,174-5.
35. Guignet EG, Hovius R, Vogel H. Reversible site-selective labeling of membrane proteins in live cells. *Nat Biotechnol* 2004; 22:440-4.
36. Lata S, Gavutis M, Tampe R, Piehler J. Specific and stable fluorescence labeling of histidine-tagged proteins for dissecting multi-protein complex formation. *J Am Chem Soc* 2006; 128:2365-72.
37. Meyer BH, Segura JM, Martinez KL, Hovius R, George N, Johnsson K, et al. FRET imaging reveals that functional neurokinin-1 receptors are monomeric and reside in membrane microdomains of live cells. *Proc Natl Acad Sci USA* 2006; 103:2138-43.
38. Grecco HE, Lidke KA, Heintzmann R, Lidke DS, Spagnuolo C, Martinez OE, et al. Ensemble and single particle photophysical properties (two-photon excitation, anisotropy, FRET, lifetime, spectral conversion) of commercial quantum dots in solution and in live cells. *Microsc Res Tech* 2004; 65:169-79.
39. Clapp AR, Medintz IL, Mattoussi H. Forster resonance energy transfer investigations using quantum-dot fluorophores. *Chemphyschem* 2006; 7:47-57.
40. Treanor B, Lanigan PM, Kumar S, Dunsby C, Munro I, Auksoorus E, et al. Microclusters of inhibitory killer immunoglobulin-like receptor signaling at natural killer cell immunological synapses. *J Cell Biol* 2006; 174:153-61.
41. Ng T, Squire A, Hansra G, Bornancin F, Prevostel C, Hanby A, et al. Imaging protein kinase Calpha activation in cells. *Science* 1999; 283:2085-9.
42. Haj FG, Verveer PJ, Squire A, Neel BG, Bastiaens PI. Imaging sites of receptor dephosphorylation by PTP1B on the surface of the endoplasmic reticulum. *Science* 2002; 295:1708-11.
43. Sapsford KE, Berti L, Medintz IL. Materials for fluorescence resonance energy transfer analysis: Beyond traditional donor-acceptor combinations. *Angew Chem Int Ed* 2006; 45:4562-88.
44. Kubitscheck U, Kircheis M, Schweitzer-Stenner R, Dreybrodt W, Jovin TM, Pecht I. Fluorescence resonance energy transfer on single living cells. Application to binding of monovalent haptens to cell-bound immunoglobulin E. *Biophys J* 1991; 60:307-18.
45. Young RM, Arnette JK, Roess DA, Barisas BG. Quantitation of fluorescence energy transfer between cell surface proteins via fluorescence donor photobleaching kinetics. *Biophys J* 1994; 67:881-8.
46. van Munster EB, Gadella TW. Fluorescence lifetime imaging microscopy (FLIM). *Adv Biochem Eng Biotechnol* 2005; 95:143-175.
47. Damjanovich S, Vereb G, Schaper A, Jenci A, Matkó J, Starink JP. Structural hierarchy in the clustering of HLA class I molecules in the plasma membrane of human lymphoblastoid cells. *Proc Natl Acad Sci USA* 1995; 92:1122-6.
48. Szabo GJ, Pine PS, Weaver JL, Kasari M, Aszalos A. Epitope mapping by photobleaching fluorescence resonance energy transfer measurements using a laser scanning microscope system. *Biophys J* 1992; 61:661-70.
49. Szabo GJ, Weaver JL, Pine PS, Rao PE, Aszalos A. Cross-linking of CD4 in a TCR/CD3-juxtaposed inhibitory state: a pFRET study. *Biophys J* 1995; 68:1170-6.
50. Jurgens L, Arndt-Jovin D, Pecht I, Jovin TM. Proximity relationships between the type I receptor for Fc epsilon (Fc epsilon RI) and the mast cell function-associated antigen (MAFA) studied by donor photobleaching fluorescence resonance energy transfer microscopy. *Eur J Immunol* 1996; 26:84-91.
51. Bacso Z, Bene L, Bodnar A, Matkó J, Damjanovich S. A photobleaching energy transfer analysis of CD8/MHC-I and LFA-1/ICAM-1 interactions in CTL-target cell conjugates. *Immunol Lett* 1996; 54:151-6.
52. Kim M, Carman CV, Springer TA. Bidirectional transmembrane signaling by cytoplasmic domain separation in integrins. *Science* 2003; 301:1720-5.
53. Patterson GH, Lippincott-Schwartz J. A photoactivatable GFP for selective photolabeling of proteins and cells. *Science* 2002; 297:1873-7.
54. Demarco IA, Periasamy A, Booker CF, Day RN. Monitoring dynamic protein interactions with photobleaching FRET. *Nat Methods* 2006; 3:519-24.
55. Youvan DC, Silva CM, Bylina EJ, Coleman WJ, Dilworth MR, Yang MM. Calibration of fluorescence resonance energy transfer in microscopy using genetically engineered GFP derivatives on nickel chelating beads. *Biotechnology et alia* 1997; 3:1-18.
56. Erickson MG, Alseikhan BA, Peterson BZ, Yue DT. Preassociation of calmodulin with voltage-gated Ca(2+) channels revealed by FRET in single living cells. *Neuron* 2001; 31:973-85.
57. Zal T, Zal MA, Gascoigne NR. Inhibition of T-cell receptor-coreceptor interactions by antagonist ligands visualized by live FRET imaging of the T-hybridoma immunological synapse. *Immunity* 2002; 16:521-34.
58. Hoppe A, Christensen K, Swanson JA. Fluorescence resonance energy transfer-based stoichiometry in living cells. *Biophys J* 2002; 83:3652-64.
59. Zal T, Gascoigne NR. Photobleaching-corrected FRET efficiency imaging of live cells. *Biophys J* 2004; 86:3923-39.
60. Gordon GW, Berry G, Liang XH, Levine B, Herman B. Quantitative fluorescence resonance energy transfer measurements using fluorescence microscopy. *Biophys J* 1998; 74:2702-13.
61. Chen H, Puhl HL, Koushik SV, Vogel SS, Ikeda SR. Measurement of FRET efficiency and ratio of donor to acceptor concentration in living cells. *Biophys J* 2006; 91:L39-41.
62. Steiner M. Changes in the distribution of platelet membrane proteins revealed by energy transfer. *Biochim Biophys Acta* 1984; 805:53-8.
63. Guo C, Dower SK, Holowka D, Baird B. Fluorescence resonance energy transfer reveals interleukin (IL)-1-dependent aggregation of IL-1 type I receptors that correlates with receptor activation. *J Biol Chem* 1995; 270:27562-8.
64. Damjanovich S, Bene L, Matkó J, Alileche A, Goldman CK, Sharrow S, et al. Preassembly of interleukin 2 (IL-2) receptor subunits on resting Kit 225 K6 T-cells and their modulation by IL-2, IL-7, and IL-15: A fluorescence resonance energy transfer study. *Proc Natl Acad Sci USA* 1997; 94:13134-9.
65. Fernandez-Miguel G, Alarcon B, Iglesias A, Bluethmann H, Alvarez-Mon M, Sanz E, et al. Multivalent structure of an alpha beta T-cell receptor. *Proc Natl Acad Sci USA* 1999; 96:1547-52.
66. Block MS, Johnson AJ, Mendez-Fernandez Y, Pease LR. Monomeric class I molecules mediate TCR/CD3 epsilon/CD8 interaction on the surface of T-cells. *J Immunol* 2001; 167:821-6.
67. Lee PU, Kranz DM. Allogeneic and syngeneic class I MHC complexes drive the association of CD8 and TCR on 2C T-cells. *Mol Immunol* 2003; 39:687-95.
68. Buslepp J, Kerry SE, Loftus D, Frelinger JA, Appella E, Collins EJ. High affinity xenoreactive TCR: MHC interaction recruits CD8 in absence of binding to MHC. *J Immunol* 2003; 170:373-83.
69. Yachi PP, Ampudia J, Gascoigne NR, Zal T. Nonstimulatory peptides contribute to antigen-induced CD8-T-cell receptor interaction at the immunological synapse. *Nat Immunol* 2005; 6:785-92.
70. Zwart W, Griekspoor A, Kuijl C, Marsman M, van Rheenen J, Janssen H, et al. Spatial separation of HLA-DM/HLA-DR interactions within MHC and phagosome-induced immune escape. *Immunity* 2005; 22:221-33.
71. Tolar P, Sohn HW, Pierce SK. The initiation of antigen-induced B-cell antigen receptor signaling viewed in living cells by fluorescence resonance energy transfer. *Nat Immunol* 2005; 6:1168-76.
72. Sohn HW, Tolar P, Jin T, Pierce SK. Fluorescence resonance energy transfer in living cells reveals dynamic membrane changes in the initiation of B-cell signaling. *Proc Natl Acad Sci USA* 2006; 103:8143-8.
73. van Rheenen J, Langeslag M, Jalink K. Correcting confocal acquisition to optimize imaging of fluorescence resonance energy transfer by sensitized emission. *Biophys J* 2004; 86:2517-29.
74. Vickery SA, Dunn RC. Scanning near-field fluorescence resonance energy transfer microscopy. *Biophys J* 1999; 76:1812-8.
75. Vickery SA, Dunn RC. Combining AFM and FRET for high resolution fluorescence microscopy. *J Microsc* 2001; 202:408-12.
76. Gadella TW Jr, Jovin TM. Oligomerization of epidermal growth factor receptors on A431 cells studied by time-resolved fluorescence imaging microscopy. A stereochemical model for tyrosine kinase receptor activation. *J Cell Biol* 1995; 129:1543-58.
77. Verveer PJ, Wouters FS, Reynolds AR, Bastiaens PI. Quantitative imaging of lateral ErbB1 receptor signal propagation in the plasma membrane. *Science* 2000; 290:1567-70.
78. Verveer PJ, Squire A, Bastiaens PI. Improved spatial discrimination of protein reaction states in cells by global analysis and deconvolution of fluorescence lifetime imaging microscopy data. *J Microsc* 2001; 202:451-456.
79. Duncan RR, Bergmann A, Cousin MA, Apps DK, Shipston MJ. Multi-dimensional time-correlated single photon counting (TCSPC) fluorescence lifetime imaging microscopy (FLIM) to detect FRET in cells. *J Microsc* 2004; 215:1-12.
80. Elangovan M, Day RN, Periasamy A. Nanosecond fluorescence resonance energy transfer-fluorescence lifetime imaging microscopy to localize the protein interactions in a single living cell. *J Microsc* 2002; 205:3-14.
81. Clegg RM, Murchie AI, Zechel A, Carlberg C, Diekmann S, Lilley DM. Fluorescence resonance energy transfer analysis of the structure of the four-way DNA junction. *Biochemistry* 1992; 31:4846-56.
82. Chen Y, Periasamy A. Characterization of two-photon excitation fluorescence lifetime imaging microscopy for protein localization. *Microsc Res Tech* 2004; 63:72-80.
83. Krishnan RV, Masuda A, Centonze VE, Herman B. Quantitative imaging of protein-protein interactions by multiphoton fluorescence lifetime imaging microscopy using a streak camera. *J Biomed Opt* 2003; 8:362-7.
84. Peter M, Ameer-Beg SM. Imaging molecular interactions by multiphoton FLIM. *Biol Cell* 2004; 96:231-6.
85. Liu Y, Walter S, Stagi M, Cherny D, Letiembre M, Schulz-Schaeffer W, et al. LPS receptor (CD14): A receptor for phagocytosis of Alzheimer's amyloid peptide. *Brain* 2005; 128:1778-89.
86. Clegg RM. FRET tells us about proximities, distances, orientations and dynamic properties. *J Biotechnol* 2002; 82:177-9.
87. Van Munster EB, Gadella TWJ. phiFLIM: a new method to avoid aliasing in frequency-domain fluorescence lifetime imaging microscopy. *J Microsc* 2004; 213:29-38.

88. Clayton AH, Hanley QS, Verveer PJ. Graphical representation and multicomponent analysis of single-frequency fluorescence lifetime imaging microscopy data. *J Microsc* 2004; 213:1-5.
89. Gertler A, Biener E, Ramanujan KV, Djiane J, Herman B. Fluorescence resonance energy transfer (FRET) microscopy in living cells as a novel tool for the study of cytokine action. *J Dairy Res* 2005; 72 Spec No:14-19.
90. Calleja V, Ameer-Beg SM, Vojnovic B, Woscholski R, Downward J, Larijani B. Monitoring conformational changes of proteins in cells by fluorescence lifetime imaging microscopy. *Biochem J* 2003; 372:33-40.
91. Suhling K, Siegel J, Phillips D, French PM, Lévêque-Fort S, Webb SE, et al. Imaging the environment of green fluorescent protein. *Biophys J* 2002; 83:3589-95.
92. McCann FE, Suhling K, Carlin LM, Eleme K, Taner SB, Yanagi K, et al. Imaging immune surveillance by T-cells and NK cells. *Immunol Rev* 2002; 2:179-92.
93. Treanor B, Lanigan PM, Suhling K, Schreiber T, Munro I, Neil MA, et al. Imaging fluorescence lifetime heterogeneity applied to GFP-tagged MHC protein at an immunological synapse. *J Microsc* 2005; 217:36-43.
94. Lidke DS, Nagy P, Barisas BG, Heintzmann R, Post JN, Lidke KA, et al. Imaging molecular interactions in cells by dynamic and static fluorescence anisotropy (rFLIM and emFRET). *Biochem Soc Trans* 2003; 31:1020-7.
95. Cohen-Kashi M, Moshkov S, Zurgil N, Deutsch M. Fluorescence resonance energy transfers measurements on cell surfaces via fluorescence polarization. *Biophys J* 2002; 83:1395-1402.
96. Harpur AG, Wouters FS, Bastiaens PI. Imaging FRET between spectrally similar GFP molecules in single cells. *Nat Biotechnol* 2001; 19:167-9.
97. Squire A, Verveer PJ, Rocks O, Bastiaens PI. Red-edge anisotropy microscopy enables dynamic imaging of homo-FRET between green fluorescent proteins in cells. *J Struct Biol* 2004; 147:62-9.
98. Clayton AH, Hanley QS, Arndt-Jovin DJ, Subramaniam V, Jovin TM. Dynamic fluorescence anisotropy imaging microscopy in the frequency domain (rFLIM). *Biophys J* 2002; 83:1631-49.
99. Mattheyses AL, Hoppe AD, Axelrod D. Polarized fluorescence resonance energy transfer microscopy. *Biophys J* 2004; 87:2787-97.
100. Rizzo MA, Piston DW. High-contrast imaging of fluorescent protein FRET by fluorescence polarization microscopy. *Biophys J* 2005; 88:L14-16.
101. Wallrabe H, Periasamy A. Imaging protein molecules using FRET and FLIM microscopy. *Curr Opin Biotechnol* 2005; 16:19-27.
102. Stockholm D, Bartoli M, Sillon G, Bourg N, Davoust J, Richard I. Imaging calpain protease activity by multiphoton FRET in living mice. *J Mol Biol* 2005; 346:215-22.
103. Zal MA, Nelson M, Zal T. Interleaved dual-wavelength multiphoton imaging system for heterologous FRET and versatile fluorescent protein excitation. *Proceedings of SPIE* 2007; 6442.
104. Tertoolen LG, Blanchetot C, Jiang G, Overvoorde J, Gadella TW Jr, Hunter T, et al. Dimerization of receptor protein-tyrosine phosphatase alpha in living cells. *BMC Cell Biol* 2001; 2:8.
105. Bhatia S, Edidin M, Almo SC, Nathenson SG. Different cell surface oligomeric states of B7-1 and B7-2: Implications for signaling. *Proc Natl Acad Sci USA* 2005; 102:15569-74.
106. Wallrabe H, Stanley M, Periasamy A, Barroso M. One- and two-photon fluorescence resonance energy transfer microscopy to establish a clustered distribution of receptor-ligand complexes in endocytic membranes. *J Biomed Opt* 2003; 8:339-46.
107. Wallrabe H, Chen Y, Periasamy A, Barroso M. Issues in confocal microscopy for quantitative FRET analysis. *Microsc Res Tech* 2006; 69:196-206.
108. Wirz SA, Davis CN, Lu X, Zal T, Bartfai T. Homodimerization and internalization of galanin type 1 receptor in living CHO cells. *Neuropeptides* 2005; 39:535-46.
109. Clayton AH, Walker F, Orchard SG, Henderson C, Fuchs D, Rothacker J, et al. Ligand-induced dimer-tetramer transition during the activation of the cell surface epidermal growth factor receptor-A multidimensional microscopy analysis. *J Biol Chem* 2005; 280:30392-9.
110. Tenhumberg S, Schuster B, Zhu L, Kovaleva M, Scheller J, Kallen KJ, et al. gp130 dimerization in the absence of ligand: preformed cytokine receptor complexes. *Biochem Biophys Res Commun* 2006; 346:649-57.
111. Kramer JM, Yi L, Shen F, Maitra A, Jiao X, Jin T, et al. Evidence for ligand-independent multimerization of the IL-17 receptor. *J Immunol* 2006; 176:711-5.
112. Krause CD, Mei E, Xie J, Jia Y, Bopp MA, Hochstrasser RM, et al. Seeing the light: Preassembly and ligand-induced changes of the interferon gamma receptor complex in cells. *Mol Cell Proteomics* 2002; 1:805-15.
113. Krause CD, Mei E, Mirochnitchenko O, Lavnikova N, Xie J, Jia Y, et al. Interactions among the components of the interleukin-10 receptor complex. *Biochem Biophys Res Commun* 2006; 340:377-85.
114. Nazarov PV, Koehorst RB, Vos WL, Apanasovich VV, Hemminga MA. FRET study of membrane proteins: determination of the tilt and orientation of the N-terminal domain of M13 major coat protein. *Biophys J* 2007; 92:1296-1305.
115. Mittler RS, Goldman SJ, Spitalny GL, Burakoff SJ. T-cell receptor-CD4 physical association in a murine T-cell hybridoma: induction by antigen receptor ligation. *Proc Natl Acad Sci USA* 1989; 86:8531-5.
116. Yachi PP, Ampudia J, Zal T, Gascoigne NR. Altered peptide ligands induce delayed CD8-T-Cell receptor Interaction-a role for CD8 in distinguishing antigen quality. *Immunity* 2006; 25:203-11.
117. Matko J, Edidin M. Energy transfer methods for detecting molecular clusters on cell surfaces. *Methods Enzymol* 1997; 278:444-62.
118. Grailhe R, Merola F, Ridard J, Couvignou S, Le Poupon C, Changeux JP, et al. Monitoring protein interactions in the living cell through the fluorescence decays of the cyan fluorescent protein. *Chemphyschem* 2006; 7:1442-54.
119. Glebov OO, Nichols BJ. Lipid raft proteins have a random distribution during localized activation of the T-cell receptor. *Nat Cell Biol* 2004; 6:238-43.
120. Sharma P, Varma R, Sarasij RC, Ira, Gousset K, Krishnamoorthy G, et al. Nanoscale organization of multiple GPI-anchored proteins in living cell membranes. *Cell* 2004; 116:577-89.
121. Matko J, Bodnar A, Vereb G, Bene L, Vámosi G, Szentesi G, et al. GPI-microdomains (membrane rafts) and signaling of the multi-chain interleukin-2 receptor in human lymphoma/leukemia T-cell lines. *Eur J Biochem* 2002; 269:1199-1208.
122. Vámosi G, Bodnar A, Vereb G, Jenei A, Goldman CK, Langowski J, et al. IL-2 and IL-15 receptor alpha-subunits are coexpressed in a supramolecular receptor cluster in lipid rafts of T-cells. *Proc Natl Acad Sci USA* 2004; 101:11082-7.
123. Nagy P, Vereb G, Sebestyen Z, Horváth G, Lockett SJ, Damjanovich S, et al. Lipid rafts and the local density of ErbB proteins influence the biological role of homo- and heteroassociations of ErbB2. *J Cell Sci* 2002; 115:4251-62.
124. Kiskowski MA, Kenworthy AK. In silico characterization of resonance energy transfer for disk-shaped membrane domains. *Biophys J* 2007; 92:3040-51.
125. Nazarov PV, Koehorst RB, Vos WL, Apanasovich VV, Hemminga MA. FRET study of membrane proteins: Simulation-based fitting for analysis of membrane protein embedment and association. *Biophys J* 2006; 91:454-66.
126. You X, Nguyen AW, Jabaiah A, Sheff MA, Thorn KS, Daugherty PS. Intracellular protein interaction mapping with FRET hybrids. *Proc Natl Acad Sci USA* 2006; 103:18458-63.
127. Lakowicz JR. *Principles of Fluorescence Spectroscopy*. New York: Plenum Publishing Corporation; 1999.
128. Matyus L, Szollosi J, Jenei A. Steady-state fluorescence quenching applications for studying protein structure and dynamics. *J Photochem Photobiol B* 2006; 83:223-36.